

## Voltage Stability Study of the Iraqi Power Grid

Dr.Rashid H. Al-Rubayi 

Electrical Engineering Department, University of Technology/Baghdad

Humam A. Al-Baidhani

Electrical Engineering Department, University of Technology/Baghdad

Email: [humam.1986@yahoo.com](mailto:humam.1986@yahoo.com)

Received on: 14/ 12/2011 & Accepted on: 21/ 7/ 2011

### ABSTRACT

It has become an important task for many voltage stability studies to find a voltage stability index. The voltage stability indices provide reliable information about proximity of voltage instability in a power system. In this paper, the L indicator has been proposed, which aims to detect the weakest load buses in the electrical power networks. The L indicator has been checked by its application to the (WSCC 9-bus and IEEE 14-bus) test systems. Finally, the proposed indicator has been applied to the Iraqi power grid (400 kV) considering different contingencies, such as lines outage, generated power reduction and loading increase. The short computation time of this indicator and its efficient detection of the weakest load buses in the Iraqi power grid, allow the operators to apply it in on-line voltage stability monitoring based on measurements.

**Keywords:** steady state voltage stability, voltage collapse, voltage stability indices and L indicator.

### دراسة استقرارية الفولتية لشبكة القدرة العراقية

#### الخلاصة

أن أيجاد دليل لاستقرارية الفولتية في العديد من الدراسات المتعلقة في استقرارية الفولتية قد أصبح من المهام الضرورية. أن هذه الدلائل تعطي معلومات وثيقة عن مدى اقتراب نظام القدرة من عدم استقرارية الفولتية. في هذا البحث، تم اقتراح الدليل (L indicator)، والذي يهدف إلى الكشف عن قضبان الأحمال الضعيفة في شبكات القدرة الكهربائية. لقد تم التحقق من الدليل (L indicator) بتطبيقه على منظومتي الاختبار (WSCC 9-bus) و (IEEE 14-bus). أخيراً، تم تطبيق الدليل المقترح على شبكة القدرة العراقية فائقة الفولتية (400 كيلو فولت) مع أخذ بعض الحالات الطارئة بنظر الاعتبار كخروج خط نقل من الخدمة وحدث نقص في توليد القدرة و زيادة الأحمال. أن زمن الحساب القصير لهذا الدليل وكفاءته في تشخيص العقد الضعيفة لشبكة القدرة الكهربائية العراقية تتيح للمشغلين بتطبيقه لمراقبة استقرارية الفولتية أيضاً اعتماداً على القياسات.

## INTRODUCTION

To operate the system with an adequate security margin, it is essential to estimate the voltage stability margin corresponding to the given operating point. The main problem here is that the maximum permissible loading of the transmission system is not a fixed quantity. It depends on various factors such as network topology, availability of reactive power support, generation and load patterns etc. All these factors continuously vary with time. Voltage magnitude alone cannot be used as an indicator of instability [1].

An accurate knowledge of how close the actual system's operating point is from the voltage stability limit is crucial to operators. Therefore, to find a voltage stability index has become an important task for many voltage stability studies. These indices provide reliable information about proximity of voltage instability in a power system. Some of the most common voltage stability indices are PV and QV curves [2], eigenvalues decomposition [3], singular values [4, 5], L indicator [6],  $dS/dY$  index [7], Voltage Collapse Proximity Indicator VCPI [8], performance index PI [9], etc.

It is necessary to choose a fast and simple indicator which at the expense of accuracy can be applied to the power system on-line to predict the voltage instability or the proximity of a collapse.

However, the L indicator (or L index) which is derived from the basic Kirchhoff laws has a simple formulation. The advantage of the L indicator method lies in the simple numerical calculation and strong adaptation in steady state and transient process. Through this indicator of voltage stability, it is easy to find the most vulnerable area in a power system. In addition, the L indicator has a very short computation time, so it is more suitable for on-line voltage stability monitoring based on measurements [10].

## VOLTAGE STABILITY ASSESSMENT USING L INDICATOR

The L indicator proposed by P. Kessel and H. Glavitsch in [6] varies in the range between zero (no load) and one (voltage collapse). Load flow solutions with a stability L indicator close to 1 are also close to singularities of the Jacobian. The calculation of the L indicator is based on the basic Kirchhoff-laws.

The L indicator that describes the voltage stability of a load bus j is given by:

$$L_j = \frac{S_{jt}^*}{V_j^2 * \bar{Y}} \quad \dots (1)$$

Where

$\bar{Y}_{jj}$  : the inverse of  $\bar{Z}_{jj}$  which can be obtained from the partial inversion of the Y-matrix.

$S_{jtot}^*$ : the apparent load power at bus j itself and the contribution of other load buses connected to it, which can be calculated from the following equation:

$$S_{jtot}^* = S_j^* + \beta \quad \dots (2)$$

Where,

$$\beta = \sum_{\substack{i \in L \\ i \neq j}} \frac{\bar{Z}_{ji} S_i^*}{\bar{Z}_{jj} V_i^*} V_j^* \quad \dots (3)$$

For the system, the vulnerable load bus must have the maximum L indicator value.

$$L_{\text{system}} = \text{Max}(L_i) \quad \dots (4)$$

Where  $i \in \text{Load}$

For large power system, the Newton-Raphson method is found to be the most efficient and practical. The number of iterations required to obtain a solution is independent of the system size, but more functional evaluations are required at each iteration. The polar form of the power flow Newton-Raphson formulation is [11]:

$$\begin{bmatrix} \Delta P \\ \Delta Q \end{bmatrix} = \begin{bmatrix} J_{11} & J_{12} \\ J_{21} & J_{22} \end{bmatrix} \begin{bmatrix} \Delta \delta \\ \Delta V \end{bmatrix} \quad \dots (5)$$

In this work, the required data for N-R program are bus data and line data, which are needed to perform repeated load flow solution in order to obtain voltage, phase, active and reactive power of the system load buses.

### CASE STUDIED RESULTS AND DISCUSSION

In this section, two test systems have been considered: the WSCC 9-bus and IEEE 14-bus test systems. The one line diagram of the WSCC 9-bus test system is shown in Fig. (1), the bus data and line data of this system are given in [12]. The simulation has been done with a MATLAB-based Power flow program solution by Newton-Raphson method (MATLAB version 7.9). The flow chart that used for the simulation has been given in Fig. (2).

The validity of this indicator has been verified by comparing the simulated result for bus 5 of the WSCC 9-bus test system with reference [12] as shown in Fig. (3), where very close results have been obtained. The L indicators of bus 5, 7 and 9 have been plotted together with individual loading increase, as shown in Fig. (4). It has been noticed that bus 5 is the most vulnerable load bus in this system, because it has the maximum indicator values as compared with other load buses.

The IEEE 14-bus test system also has been studied to ensure the validity of this indicator to detect the weakest load bus. The one line diagram is shown in Fig. (5), the line data and bus data of this network are given in [13]. Fig. (6) shows the simulated plots of L indicators for all load buses with individual loading increase.

The simulated plots show that bus 14 is the weakest load bus, because it has the maximum indicator values as compared with other load buses.

### THE IRAQI POWER GRID (400 KV) CASE STUDY

In this section, the application of the L indicator has been studied to the Iraqi power grid (400 kV), considering different contingencies (loading increase, line outage and reduction in the generated power). Fig. (7) shows a configuration of this network. The bus data and line data are given in table (1) and table (2), respectively [14].

The results have been obtained considering two constraints through loading increase:

- The slack bus (MUSP) power must not exceed the maximum generation limit (1200 MW).
- The voltage magnitude at load buses must not decrease below 0.9 p.u.

Notes:

- ✓ The load has been increased at the load buses in each case with constant power factor of (0.86).
- ✓ The two constraints are considered for cases 2 and 3 only.

### CASES STUDIED

Case 1:

a) Increasing load at all load buses individually from zero to the collapse point. Fig. (8) shows the plots of indicator curves for all load buses. The results obtained in this case show that buses 16 (QIM4), 23 (KUT4) and 24 (AMR4) are the weakest load buses, because they have the maximum L indicator values.

The weakest buses 16 (QIM4), 23 (KUT4) and 24 (AMR4) have been plotted together in Fig. (9). It can be noticed that buses 16, 23 and 24 have the lowest self admittance values  $Y_{jj}$  as compared with other load buses; this will restrict the power transferred to these load buses through transmission lines that connected to them, so their L indicator values will be increased. As a result, they become the weakest load buses in the Iraqi power grid (400 kV).

Case 2:

Increasing load at each load bus individually from zero to the point at which one of the two constraints has been violated, adding the effect of lines outage to the resulting indicator values. Table (3) shows the simulated results.

Case 3:

Repeat case 2, adding the effect of generated power reduction of one voltage-controlled bus to 75% of its nominal value. The simulated results are shown in table (4). It can be noticed that the Iraqi power grid system is heavily loaded, so any more reduction in the generated power at one PV bus below 75% will make the slack bus (MUSP) unable to meet the loading increase that occurs at the load buses.

---

Results of cases 2 and 3 show that bus 23 (KUT4) is the weakest load bus, because they have the maximum L indicator values with minimum voltage magnitudes. This is attributed to the same reasons mentioned in case 1.

### **CONCLUSIONS**

The conclusions from this work can be summarized as follows:

- 1) A voltage stability indicator has been implemented, which has been used to detect the weakest load buses in the electrical networks.
- 2) The L indicator algorithm has been verified by its implementation to the WSCC 9-bus and IEEE 14-bus test systems to detect the weakest load buses. The results conform these of reference [12].
- 3) The application of the L indicator to the Iraqi power grid (400 kV) has been studied. Many contingencies have been considered, lines outage, generated power reduction and loading power increase. The weakest load bus has been determined successfully at each case.
- 4) All the results obtained from system simulation show the ability of L indicator to detect the weakest load bus in the electrical networks. In addition, the short computation time and the simple formulation of the indicator will enable it to be used in the on-line voltage stability monitoring.

### **REFERENCES**

- [1] Bergovic, K. Vu, M. M. D. Novosel, M. M. Saha, "Use of local measurements to estimate voltage stability margin", IEEE transactions of power systems, Vol. 14, No. 3, Aug 1999.
- [2] Asnal Effendi, Sasongko Pramono Hadi, Soedjatmiko, "Voltage stability analysis of power system electrical apply to sumbagteng system (sumbar-riau-jambi)", Institut Teknologi Bandung, Indonesia June 17-19, 2007.
- [3] Claudio A. Canizares, Antonio C. Z. de Souza, Victor H. Quintana, "Comparison of performance indices for detection of proximity to voltage collapse", IEEE Transactions on Power Systems, Vol. 11, No. 3, August 1996.
- [4] Andersson, P-A Löf, G. D. J. Hill, "Voltage stability indices for stressed power systems", IEEE Transactions on Power Systems, Vol. 8, No. 1, February 1993.
- [5] Löf, P-A T. Smed, G. Andersson, D. J. Hill, "Fast calculation of a voltage stability index", Transactions on Power Systems, Vol. 7, No. 1, February 1992.
- [6] P. Kessel. and H. Glavitch, "Estimating the voltage stability of a power system", IEEE Transaction on Power Deliver, Vol. PWRD-1, No.3. pp.346-354. July 1986.
- [7] Phadk, A. R. e, Manoj Fozdar, K. R. Niazi, "A New technique for on-line monitoring of voltage stability margin using local signals", Fifteenth National Power Systems Conference (NPSC), IIT Bombay, December 2008.
- [8] Yuan-Lin Chen, Chi-Wei Chang, Chun-Chang Liu, "Efficient methods for identifying weak nodes in electrical power networks", IEE Proceeding – Generation, Transmission and Distribution, Vol. 142, No. 3, May 1995.

- [9] Mário A. Albuquerque, Carlos A. Castro, “A Contingency ranking method for voltage stability in real time operation of power systems”, IEEE Bologna Power Tech Conference, Bologna, Italy, 2003.
- [10] Garng M. Huang, Liang Zhao, “Measurement based voltage stability monitoring of power system”, Department of Electrical Engineering, Texas A & M University, 2002.
- [11] Haadi Saadat, “Power System Analysis”, by McGraw-Hill, 1999.
- [12] Garng M. Huang, Ali Abur, “Voltage security margin assessment”, Texas A&M University, PSERC Publication 02-49, December 2002 .
- [13] Raúl Bachiller Prieto, “Optimal market settlements incorporating voltage stability considerations and FACTS devices”, M.Sc. thesis submitted to the Department of Energy and Environment Division of Electric Power Engineering at Chalmers University of Technology, Göteborg, Sweden, 2008.
- [14] National Dispatch Center (NDC), Baghdad, Iraq, 2010.

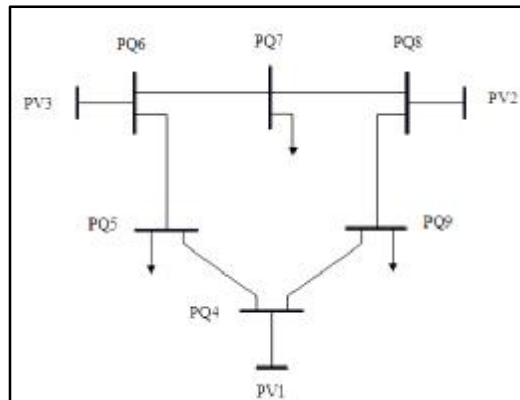


Figure (1):The one line diagram of WSCC 9-bus test svstem

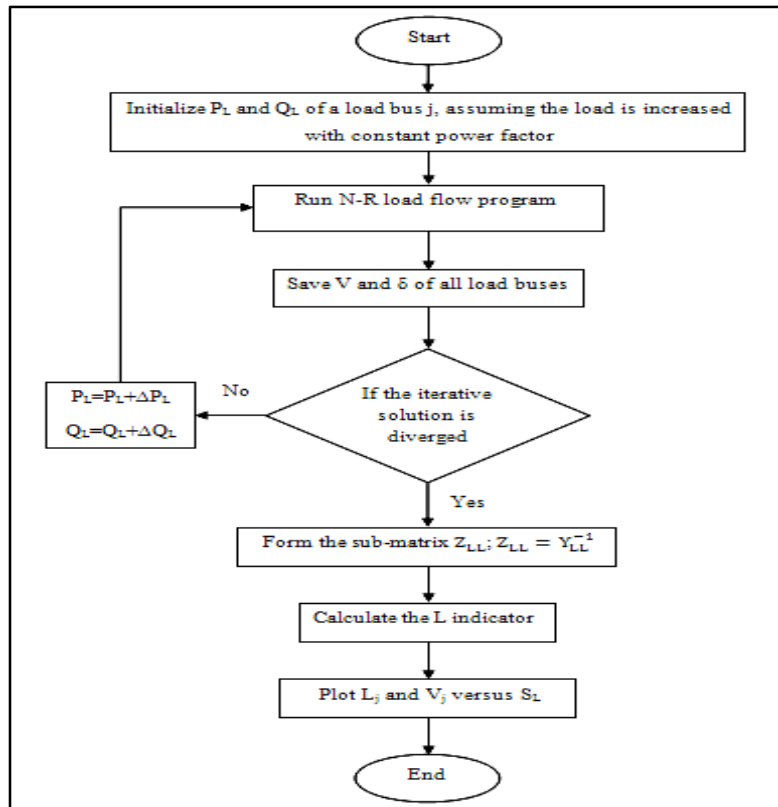


Figure (2): Flow chart of L indicator calculation.

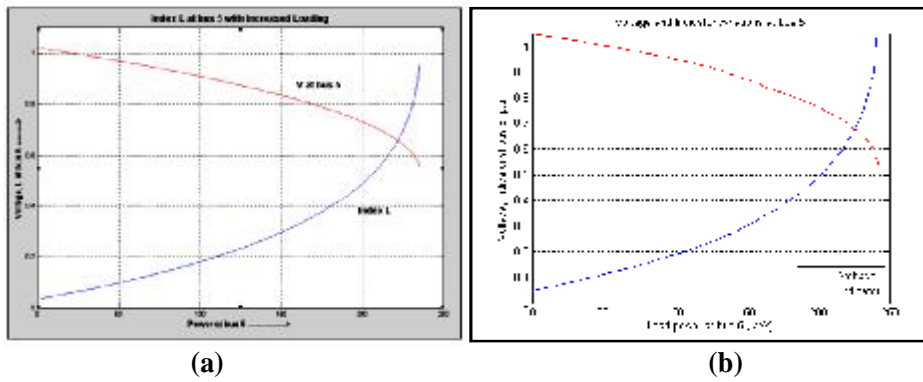


Figure (3): Results comparison of bus 5 (WSCC 9-bus) : (a) Result of reference [12], (b) Simulated result

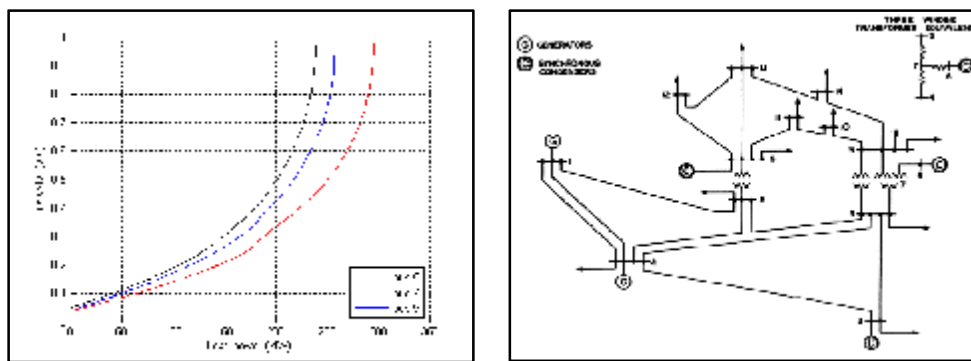


Figure (4): Indicator curves of buses 5, 7 and 9 (WSCC 9-bus) with individual increased loading.

Figure (5): The one line diagram of IEEE 14-bus test system

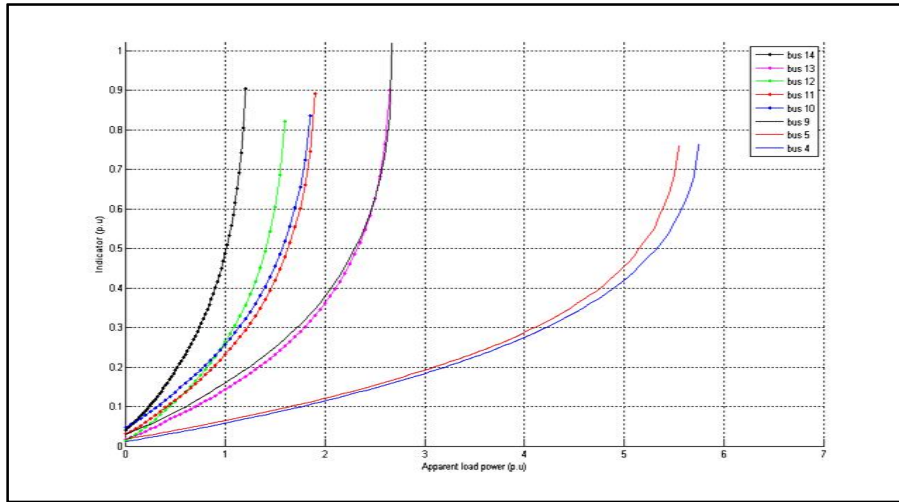


Figure (6): Indicator curves of all load buses (IEEE 14-bus) with individual loading.

Table (1): bus data of the Iraqi power grid (400 kV)

Bus Number	Bus Name	Voltage (pu)	$P_L$ (MW)	$Q_L$ (Mvar)	$P_G$ (MW)
1	MUSP	1.0400	199.7795	116.6333	1107.1
2	MMDH	1.0200	000.0000	000.0000	690.10
3	BAJP	1.0250	124.8622	092.2467	406.00
4	BAJG	1.0250	000.0000	000.0000	590.45
5	KRK4	1.0217	129.8567	60.48960	239.87
6	MUSG	1.0400	000.0000	000.0000	369.00
7	HDTH	1.0300	253.0540	075.6120	202.97
8	QDSG	1.0075	000.0000	000.0000	735.30
9	KAZG	1.0096	566.0419	294.6579	207.58
10	HRTF	1.0150	154.8291	072.1171	332.13
11	NSRP	1.0197	422.8665	198.3219	775.00
12	DYL4	1.0000	83.24150	021.1712	000.00
13	BGW4	1.0000	576.0310	302.4481	000.00
14	BGN4	1.0000	412.8776	139.1261	000.00
15	BGE4	1.0000	849.0627	294.6579	000.00
16	QIM4	1.0000	109.8787	039.3182	000.00
17	BGC4	1.0000	49.94490	181.4688	000.00
18	BGS4	1.0000	000.0000	000.0000	000.00
19	AMN4	1.0000	126.5640	056.0014	184.52
20	MSL4	1.0000	649.2833	302.4481	000.00
21	BAB4	1.0000	307.9934	184.6695	000.00
22	KDS4	1.0000	213.0981	151.4458	000.00
23	KUT4	1.0000	259.7134	108.1756	000.00
24	AMR4	1.0000	311.0221	160.3709	000.00

Table (2): line data of the Iraqi power grid (400 kV)

From Bus	To Bus	Line R (pu)	Line X (pu)	Charging (pu)
20	2	0.00144	0.01177	0.36439
20	2	0.00144	0.01177	0.36439
20	3	0.0042	0.03437	1.06426
20	3	0.0042	0.03437	1.06426
3	4	0.00002	0.0002	0.00584
3	13	0.00483	0.04393	1.30165
3	13	0.00496	0.04511	1.33667
3	7	0.00345	0.03132	0.92808
4	5	0.0018	0.01635	0.48447
5	15	0.005114	0.046492	1.377532
5	12	0.004247	0.038612	1.144052
13	14	0.00093	0.00847	0.25099
13	17	0.000616	0.005608	0.166179
13	7	0.00485	0.04405	1.30515
18	19	0.00082	0.00749	0.22181
18	19	0.00082	0.00749	0.22181
18	17	0.000964	0.008772	0.259921
18	1	0.00122	0.01015	0.31897
18	6	0.001094	0.009106	0.286176
18	22	0.00308	0.02795	0.82827
15	14	0.00029	0.00262	0.07763
15	19	0.00043	0.00394	0.11674
15	19	0.00043	0.00394	0.11674
15	12	0.00087	0.00788	0.23348
14	8	0.00015	0.00138	0.04086
14	8	0.00015	0.00138	0.04086
19	23	0.02744	0.22904	0.09156
23	11	0.00432	0.03928	1.1639
23	24	0.00479	0.04354	1.28998
7	16	0.00292	0.02391	0.74035
1	6	0.000125	0.001043	0.032791
1	21	0.00081	0.00673	0.21165
1	21	0.00081	0.00673	0.21165
21	22	0.00233	0.01935	0.60812
21	22	0.00233	0.01935	0.60812
22	11	0.00383	0.03485	1.03256
11	9	0.00439	0.03993	1.18316
24	10	0.0029	0.0264	0.78216
10	9	0.00118	0.01076	0.3187
10	9	0.00118	0.01076	0.3187

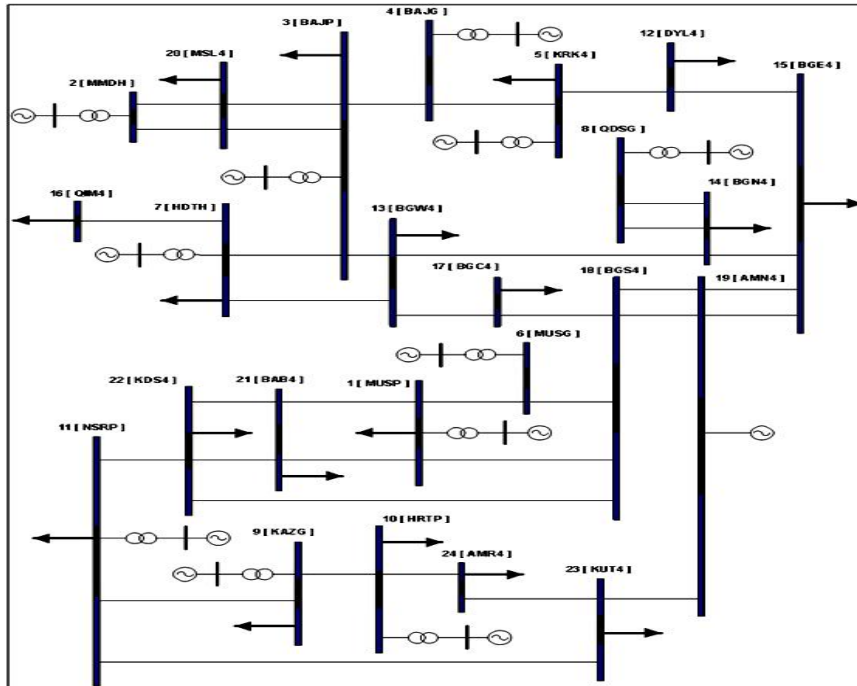


Figure (7): configuration of the Iraqi super power grid (400

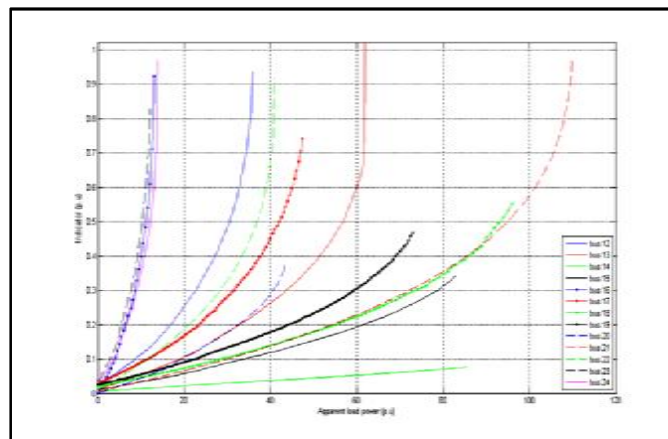


Figure (8): Indicator curves of all load buses with individual loading increase

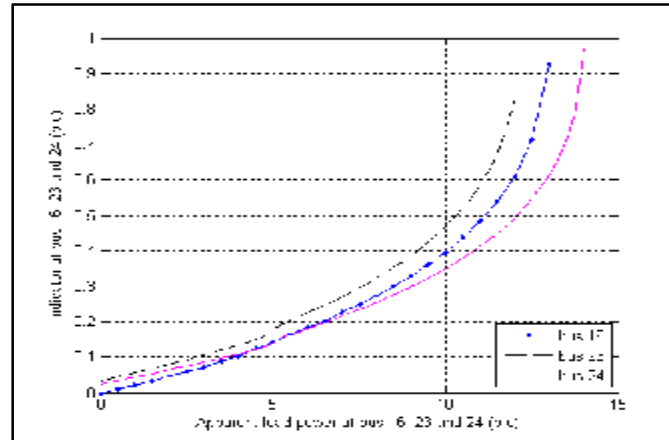


Figure (9): Indicator curves of the weakest load buses with individual loading increase

Table (3): The effect of lines' outage on the resulting L

		Number Of The Outage Line															
		13-14		13-17		14-15		15-19		17-18		18-19		18-22		19-23	
Bus No.	Bus Name	V (p.u)	L (p.u)	V (p.u)	L (p.u)	V (p.u)	L (p.u)	V (p.u)	L (p.u)	V (p.u)	L (p.u)	V (p.u)	L (p.u)	V (p.u)	L (p.u)	V (p.u)	L (p.u)
12	DAL4	1.005	0.0445	1.005	0.0443	1.003	0.0919	1.004	0.0449	1.006	0.0435	1.003	0.0462	1.005	0.0444	1.005	0.0441
13	BGW4	0.997	0.0800	0.999	0.0510	1.002	0.0492	1.002	0.0462	0.989	0.0601	1.003	0.0459	1.002	0.0460	1.002	0.0460
14	BGN4	1.005	0.0101	1.005	0.0121	1.005	0.0074	1.005	0.0120	1.005	0.0124	1.005	0.0123	1.005	0.0119	1.006	0.0118
15	BGE4	1.001	0.0360	1.002	0.0358	0.991	0.0987	1.000	0.0366	1.003	0.0349	0.999	0.0381	1.001	0.0358	1.002	0.0355
16	QIM4	1.002	0.0630	1.002	0.0630	1.002	0.0630	1.002	0.0630	0.991	0.0643	1.002	0.0630	1.002	0.0630	1.003	0.0604
17	BGC4	1.013	0.0592	1.019	0.0384	1.013	0.0494	1.013	0.0401	0.995	0.0654	1.013	0.0393	1.012	0.0399	1.013	0.0400
18	BGS4	1.021	0.0284	1.021	0.0237	1.021	0.0437	1.022	0.0243	1.026	0.0200	1.023	0.0229	1.020	0.0238	1.021	0.0239
19	AMN4	1.010	0.0354	1.010	0.0335	1.009	0.0775	1.012	0.0343	1.012	0.0317	1.006	0.0375	1.009	0.0337	1.010	0.0332
20	MSL4	1.005	0.0396	1.005	0.0396	1.005	0.0396	1.005	0.0396	1.005	0.0396	1.005	0.0396	1.005	0.0396	1.005	0.0396
21	BAB4	1.031	0.0203	1.031	0.0200	1.031	0.0213	1.031	0.0201	1.032	0.0197	1.031	0.0200	1.030	0.0211	1.031	0.0201
22	KDS4	1.023	0.0404	1.023	0.0392	1.023	0.0442	1.023	0.0394	1.024	0.0381	1.024	0.0390	1.018	0.0458	1.022	0.0394
23	KUT4	<b>0.968</b>	<b>0.1421</b>	<b>0.968</b>	<b>0.1419</b>	<b>0.968</b>	<b>0.1457</b>	<b>0.968</b>	<b>0.1418</b>	<b>0.968</b>	<b>0.1416</b>	<b>0.968</b>	<b>0.1422</b>	<b>0.967</b>	<b>0.1420</b>	<b>0.918</b>	<b>0.1687</b>
24	AMR4	<b>0.954</b>	<b>0.1349</b>	<b>0.954</b>	<b>0.1348</b>	<b>0.963</b>	<b>0.1341</b>	<b>0.963</b>	<b>0.1326</b>	<b>0.963</b>	<b>0.1325</b>	<b>0.954</b>	<b>0.1350</b>	<b>0.943</b>	<b>0.1380</b>	<b>0.932</b>	<b>0.1433</b>

**Table (4): The effect of generated power reduction on the resulting**

		The Names Of PV Buses At Which The Generated Power Is Reduced To 75% Of Its Nominal Value											
		BAJP		KRK4		MUSG		HDTH		KRZG		HRTH	
Bus No.	Bus Name	V (p.u)	L (p.u)	V (p.u)	L (p.u)	V (p.u)	L (p.u)	V (p.u)	L (p.u)	V (p.u)	L (p.u)	V (p.u)	L (p.u)
12	DAL4	1.010	0.0362	1.008	0.0404	1.010	0.0362	1.007	0.0404	1.007	0.0404	1.010	0.0362
13	BGW4	1.005	0.0417	1.004	0.0439	1.005	0.0417	1.004	0.0439	1.004	0.0440	1.005	0.0417
14	BGN4	1.006	0.0110	1.006	0.0113	1.006	0.0110	1.006	0.0113	1.006	0.0113	1.006	0.0113
15	BGE4	1.003	0.0333	1.003	0.0342	1.003	0.0337	1.002	0.0346	1.002	0.0347	1.003	0.0337
16	QIM4	1.020	0.0327	1.013	0.0450	1.019	0.0351	1.011	0.0475	1.011	0.0475	1.017	0.0376
17	BGC4	1.016	0.0344	1.014	0.0373	1.016	0.0344	1.014	0.0373	1.014	0.0373	1.016	0.0344
18	BGS4	1.023	0.0219	1.022	0.0231	1.023	0.0219	1.022	0.0231	1.022	0.0231	1.023	0.0219
19	AMN4	1.012	0.0311	1.011	0.0326	1.012	0.0311	1.011	0.0326	1.011	0.0326	1.012	0.0311
20	MSL4	1.007	0.0350	1.006	0.0373	1.007	0.0350	1.006	0.0373	1.006	0.0373	1.007	0.0350
21	BAB4	1.033	0.0172	1.032	0.0186	1.033	0.0172	1.032	0.0186	1.032	0.0186	1.033	0.0172
22	KDS4	1.028	0.0321	1.025	0.0358	1.028	0.0321	1.025	0.0358	1.025	0.0358	1.027	0.0322
23	KUT4	<b>0.986</b>	<b>0.1129</b>	<b>0.979</b>	<b>0.1242</b>	<b>0.984</b>	<b>0.1157</b>	<b>0.977</b>	<b>0.1271</b>	<b>0.939</b>	<b>0.1353</b>	<b>0.954</b>	<b>0.1234</b>
24	AMR4	<b>0.986</b>	<b>0.1059</b>	<b>0.980</b>	<b>0.1156</b>	<b>0.986</b>	<b>0.1059</b>	<b>0.979</b>	<b>0.1180</b>	<b>0.942</b>	<b>0.1249</b>	<b>0.940</b>	<b>0.1181</b>